

Syntheses, crystal structures and vibrational spectra of $KLn(SO_4)_2 \cdot H_2O$ ($Ln=La, Nd, Sm, Eu, Gd, Dy$)

Karolina Kazmierczak, Henning A. Höppe*

Institut für Anorganische und Analytische Chemie, Albert-Ludwigs-Universität, Albertstraße 21, D-79104 Freiburg, Germany

1. Introduction

Lanthanide compounds play a very important role in materials science. Trivalent lanthanide ions can act as a quantum cutter (downconversion) or induce high-energy photons from low-energy photons (upconversion). They are also interesting for the production of efficient fluorescent materials [1,2]. Unlike silicates and phosphates sulphates can only be synthesised at lower temperatures since they cannot be prepared from their melt due to decomposition. Thus most of the known crystal structures contain solvent molecules [3].

Several of the double sulphates of the alkali metals and lanthanide element ions with the formula $MLn(SO_4)_2 \cdot H_2O$ were characterised already [4–13]. So far, looking at the crystal structures of the monohydrated potassium compounds $KLn(SO_4)_2 \cdot H_2O$ ($Ln=Ce$ [10], Pr [11], Tb [12], Lu [13]) have been investigated. In this contribution we will describe the preparation, crystal structures – looking very carefully at structural differences – and compare the vibrational spectra of the potassium lanthanide double sulphates monohydrates $KLn(SO_4)_2 \cdot H_2O$ ($Ln=La, Nd, Sm, Eu, Gd, Dy$). Moreover, selected UV-vis reflection spectra will be presented.

These monohydrates will be good candidates to obtain crystal-water free sulphates, but it is important to know the exact

compounds from which the dehydration starts, and this is the main topic of this contribution.

2. Experimental section

Synthesis of $KLn(SO_4)_2 \cdot H_2O$ ($Ln=La, Nd, Sm, Eu, Gd, Dy$): The double sulphates of $KLn(SO_4)_2 \cdot H_2O$ were prepared by mixing aqueous solutions of $Ln(SO_4)_2 \cdot H_2O$ and KSCN (Merck, pur) in the molar ratio 1:2 [10]. Colourless, acicular crystals were obtained by slow evaporation of water at room temperature after a few weeks.

Crystal structure determination of $KLn(SO_4)_2 \cdot H_2O$ ($Ln=La, Nd, Sm, Eu, Gd, Dy$): X-Ray diffraction data were collected on a Stoe IPDS 2 diffractometer – corrected numerically for absorption [14] – on a Rigaku Spider Image-Plate diffractometer and on a Bruker AXS CCD (APEX-II) diffractometer using MoK α radiation at room temperature, both corrected for absorption by applying a multi-scan correction [15,16].

The crystal structures of $KLn(SO_4)_2 \cdot H_2O$ were solved by direct methods, using SHELXTL [17]. The relevant crystallographic data are summarised in Table 1. Tables 2–7 show the atomic coordinates and displacement parameters of all atoms in $KLn(SO_4)_2 \cdot H_2O$ ($Ln=La, Sm, Eu, Gd, Dy$). Table 8 illustrates the identified hydrogen bonds, Table 9 lists selected geometric parameters of $KLn(SO_4)_2 \cdot H_2O$ ($Ln=La, Nd, Sm, Eu, Gd, Dy$).

Further details of the crystal structure investigations presented in this work maybe obtained from the Fachinformationszentrum Karlsruhe, D-76344 Eggenstein-Leopoldshafen,

* Corresponding author. Fax: +49 761 203 6012.

E-mail address: henning.hoeppe@ac.uni-freiburg.de (H.A. Höppe).

Table 1

Crystal data and parameters of the structure refinements.

	KLa(SO₄)₂·H₂O	KNd(SO₄)₂·H₂O	KSm(SO₄)₂·H₂O	KEu(SO₄)₂·H₂O	KGd(SO₄)₂·H₂O	KDy(SO₄)₂·H₂O
Temperature (K)	298(2)	298(2)	298(2)	298(2)	298(2)	298(2)
Molar weight (g/mol)	388.15	393.48	399.59	401.20	406.49	411.74
Crystal system	Trigonal	Monoclinic	Monoclinic	Monoclinic	Monoclinic	Monoclinic
Space group	<i>P</i> 3 ₂ 1	<i>P</i> 2 ₁ / <i>c</i>				
<i>a</i> (Å)	7.1490(5)	10.0500(5)	10.047(1)	10.076(2)	10.1255(15)	10.106(3)
<i>b</i> (Å)		8.5250(4)	8.4555(1)	8.4240(17)	8.3856(13)	8.2934(17)
<i>c</i> (Å)		13.2439(12)	10.3597(5)	10.349(1)	10.352(2)	10.3501(16)
<i>β</i> (Å ³)			118.486(2)	118.90 (0)	119.19(3)	119.50(2)
Cell volume (Å ³)	586.19(8)	780.12(7)	769.62(2)	767.1(3)	767.0(2)	751.0(3)
<i>Z</i>	3	4	4	4	4	4
Calculated density <i>D</i> _x (g/cm ³)	3.299	3.350	3.449	3.474	3.520	3.641
<i>μ</i> (mm ⁻¹)	6.555	7.746	8.736	9.286	9.756	11.082
<i>F</i> (0 0 0)	546	740	748	752	756	764
Radiation	MoK α radiation	MoK α radiation	MoK α radiation	MoK α radiation	MoK α radiation	MoK α radiation
Diffractometer	STOE IPDS 2	Bruker AXS CCD	Bruker AXS CCD	Rigaku Spider Image-Plate	Rigaku Spider Image-Plate	STOE IPDS 2
Absorption correction	Numerical	Multi-scan	Multi-scan	Multi-scan	Multi-scan	Numerical
Index range	-8/-8/-15 8/7/15	-11/-10/-12 11/10/11	-10/-9/-9 10/5/11	10/9/11	10/9/11	-10/-8/-11 10/8/10
Theta range (Θ_{\min} - Θ_{\max})	2.5-24.94	2.31-24.99	3.35-22.49	2.57-22.5	2.5-22.5	2.5-22.5
Reflections collected	5727	11 775	1653	4881	10 024	3437
Independent reflections	695	1125	945	995	996	964
Flack parameter χ	0.02(3)	-	-	-	-	-
<i>R</i> _{int} , <i>R</i> _{sigma}	0.055, 0.023	0.080, 0.038	0.019, 0.026	0.039, 0.029	0.136, 0.072	0.079, 0.061
<i>R</i> ₁ (all data)	0.017	0.039	0.024	0.022	0.042	0.045
w <i>R</i> ₂ (all data)	0.038	0.053	0.060	0.041	0.100	0.071
Goodness of fit (GooF)	1.024	1.018	1.182	1.052	1.079	0.971
Residual electron density, min/ max	-0.38/0.09	-0.817 /0.704	-1.42/0.19	-0.44/ 0.50	-1.24/1.64	-1.04/ 1.29

Table 2Atomic coordinates, Wyckoff symbols and isotropic displacement parameters *U*_{eq}/Å² for the atoms in KLa(SO₄)₂·H₂O.

Atom	Wyckoff symbol	<i>x</i>	<i>y</i>	<i>z</i>	<i>U</i> _{eq}
La	3a	0.56517(4)	0.56517(4)	0	0.02011(12)
K	3b	0	0.44528(17)	0.8333	0.0268(2)
S	6c	0.00479(15)	0.44137(15)	0.09185(5)	0.02082(19)
O1	6c	0.8788(4)	0.2497(4)	0.15586(19)	0.0293(6)
O2	6c	0.1154(5)	0.6225(5)	0.16322(17)	0.0299(6)
O3	6c	0.8645(5)	0.4778(5)	0.0241(2)	0.0305(7)
O4	6c	0.1609(5)	0.4144(5)	0.0306(2)	0.0303(7)
OW	3a	0.9199(8)	0.9199(8)	0	0.066(2)

Germany (e-mail: to:crysdata@fiz-karlsruhe.de) on quoting the depository numbers CSD-421804 (KLa(SO₄)₂·H₂O), CSD-421816 (KNd(SO₄)₂·H₂O), CSD-421803 (KSm(SO₄)₂·H₂O), CSD-421801 (KEu(SO₄)₂·H₂O), CSD-421802 (KGd(SO₄)₂·H₂O) and CSD-421800 (KDy(SO₄)₂·H₂O), the names of the authors, and citation of this publication.

UV-vis spectroscopy: The optical reflection spectra for KEu(SO₄)₂·H₂O and KNd(SO₄)₂·H₂O were recorded in reflection geometry using an UV-vis spectrophotometer (Cary 300 Scan, Varian) fitted with an integrating sphere and are shown in Figs. 7 and 8, respectively. The spectra were obtained from 200 to 800 nm at a scan rate of 100 nm/min.

Vibrational spectroscopy: Infrared spectra were recorded at room temperature by using a Bruker IFS 66v/S spectrometer. The samples were thoroughly mixed with dried KBr (ca. 1 mg sample, 300 mg KBr). Raman spectra were recorded by a Bruker FRA 106/S module by excitation with a Nd-YAG laser ($\lambda=1064$ nm) scanning in the range from 400 to 4000 cm⁻¹.

3. Crystal structure of KLn(SO₄)₂·H₂O with Ln=La, Nd, Sm, Eu, Gd, Dy.

The crystal structures of KLn(SO₄)₂·H₂O (*Ln*=Nd, Sm, Gd) (**1**) are isotypic with that of KCe(SO₄)₂·H₂O [10], the crystal structures of KLn(SO₄)₂·H₂O (*Ln*=Eu, Dy) (**2**) are isotypic with KLn(SO₄)₂·H₂O (*Ln*=Pr [11], Lu [13]). Projections of the structures of **1** and **2** along [0 1 0] are presented in Fig. 1.

In both structures alternating *Ln* and K atoms build hexagonal undulated layers (parallel to the *bc* layer) which are packed like in graphitic boron nitride [18]. Thus the lanthanide atoms are surrounded by five K atoms forming a distorted trigonal bipyramidal and vice versa. In this structure two different kinds of voids centred at Wyckoff position 2*d* could be identified. The large hexagonal prismatic voids (**void 1**) are occupied by two S(1)O₄²⁻ anions and two crystal water molecules each, the smaller trigonal prismatic ones (**void 2**) contain only a single S(2)O₄²⁻ anion (Fig. 2).

The potassium cations are coordinated irregularly by nine oxygen atoms in both structures (Fig. 3). Four of the nine oxygen atoms originate from monodentate sulphate ligands, four atoms from bidentate sulphate ligands and one from the crystal water molecule. The K-O distances vary between 2.767(5) and 3.172(4) Å in **1** and between 2.673(9) and 3.288(8) Å in **2**. These distances agree well with the sum of ionic radii of 2.90 Å [19]. A careful analysis of the coordination distances reveals that this also holds for the potassium ions in Ref. [10] (*Ln*=Ce).

The coordination environment of the lanthanide ions is different in the cases **1** and **2**, respectively. In **1**, the lanthanide atoms are nine-fold coordinated, each bound to eight oxygen atoms of six sulphate ligands (four monodentate, two bidentate) and a single crystal water molecule (Fig. 4a). In **2** the *Ln* ions are eight-fold coordinated by oxygen atoms (Fig. 4b) with two oxygen

Table 3

Anisotropic displacement parameters $U_{ij}/\text{\AA}^2$ for the atoms in $\text{KLa}(\text{SO}_4)_2 \cdot \text{H}_2\text{O}$.

Atom	U_{11}	U_{22}	U_{33}	U_{12}	U_{13}	U_{23}
La	0.02157(15)	0.02157(15)	0.01854(16)	-0.00002(7)	0.00002(7)	0.01179(17)
K	0.0215(6)	0.0309(5)	0.0251(5)	0.0004(3)	0.0007(5)	0.0107(3)
S	0.0197(5)	0.0225(4)	0.0197(4)	0.0002(3)	0.0002(4)	0.0102(4)
O1	0.0290(15)	0.0223(13)	0.0275(12)	0.0036(11)	0.0037(11)	0.0061(12)
O2	0.0327(16)	0.0251(14)	0.0250(14)	-0.0017(10)	-0.0012(14)	0.0094(12)
O3	0.0288(17)	0.042(2)	0.0262(12)	0.0017(12)	-0.0013(12)	0.0220(18)
O4	0.0303(14)	0.0398(16)	0.0284(14)	0.0025(12)	0.0059(12)	0.0233(12)
OW	0.032(2)	0.032(2)	0.118(6)	-0.0139(19)	0.0139(19)	0.005(3)

Table 4

Atomic coordinates, Wyckoff symbols and isotropic displacement parameters $U_{eq}/\text{\AA}^2$ for the atoms in $\text{KSm}(\text{SO}_4)_2 \cdot \text{H}_2\text{O}$.

Atom	Wyckoff symbol	x	y	z	U_{eq}
Sm	4e	0.26146(3)	0.84453(3)	0.03233(3)	0.0087(2)
K	4e	-0.21429(15)	0.81512(16)	0.30796(15)	0.0222(3)
S1	4e	0.51379(16)	1.18658(17)	0.11004(16)	0.0115(3)
O11	4e	0.5419(4)	1.3141(4)	0.2176(4)	0.0171(8)
O12	4e	0.4046(4)	1.0793(4)	0.1168(4)	0.0178(9)
O13	4e	0.6588(4)	1.1041(6)	0.1520(5)	0.0307(10)
O14	4e	0.4628(6)	1.2502(5)	-0.0363(5)	0.0423(13)
S2	4e	0.04965(15)	0.86787(16)	0.17740(15)	0.0091(3)
O21	4e	0.0715(4)	0.7875(4)	0.3108(4)	0.0146(8)
O22	4e	-0.0982(4)	0.9460(5)	0.1125(4)	0.0186(8)
O23	4e	0.0543(4)	0.7540(4)	0.0713(4)	0.0179(8)
O24	4e	0.1738(4)	0.9802(4)	0.2109(4)	0.0201(9)
OW	4e	0.3110(5)	0.5514(5)	0.0400(5)	0.0242(10)

Table 5

Anisotropic displacement parameters $U_{ij}/\text{\AA}^2$ for the atoms in $\text{KSm}(\text{SO}_4)_2 \cdot \text{H}_2\text{O}$.

Atom	U_{11}	U_{22}	U_{33}	U_{12}	U_{13}	U_{23}
Sm	0.0085(3)	0.0068(3)	0.0090(3)	0.00030(9)	0.00272(19)	-0.00069(8)
K	0.0193(7)	0.0256(7)	0.0216(7)	0.0010(6)	0.0099(6)	0.0027(5)
S1	0.0155(7)	0.0121(6)	0.0094(7)	-0.0042(6)	0.0078(6)	-0.0078(6)
O11	0.020(2)	0.0139(17)	0.015(2)	-0.0055(17)	0.0072(17)	-0.0036(16)
O12	0.0170(19)	0.014(2)	0.025(2)	-0.0053(17)	0.0126(17)	-0.0097(16)
O13	0.021(2)	0.038(2)	0.044(3)	-0.012(2)	0.024(2)	-0.003(2)
O14	0.078(4)	0.027(2)	0.012(2)	0.0035(19)	0.014(2)	-0.019(2)
S2	0.0082(7)	0.0110(7)	0.0090(7)	0.0027(5)	0.0048(6)	0.0027(5)
O21	0.0141(18)	0.017(2)	0.0133(18)	0.0041(17)	0.0068(16)	0.0040(16)
O22	0.0139(19)	0.022(2)	0.0189(19)	0.0074(17)	0.0076(16)	0.0056(16)
O23	0.0197(18)	0.0197(19)	0.0187(19)	-0.0043(17)	0.0128(16)	-0.0037(16)
O24	0.018(2)	0.018(2)	0.027(2)	0.0004(18)	0.0125(17)	-0.0024(17)
OW	0.026(2)	0.019(2)	0.024(2)	0.0030(19)	0.0096(19)	0.0086(19)

Table 6

Atomic coordinates, Wyckoff symbols and isotropic displacement parameters $U_{eq}/\text{\AA}^2$ for the atoms in $\text{KDy}(\text{SO}_4)_2 \cdot \text{H}_2\text{O}$.

Atom	Wyckoff symbol	x	y	z	U_{eq}
Dy	4e	0.74426(6)	0.35652(7)	0.46306(5)	0.0254(3)
K	4e	0.2096(4)	0.1702(4)	0.6862(3)	0.0530(9)
S1	4e	0.4980(3)	0.2009(4)	0.1007(3)	0.0279(7)
O11	4e	0.5511(9)	0.3196(9)	0.2217(8)	0.0291(19)
O12	4e	0.4021(9)	0.0870(10)	0.1251(8)	0.033(2)
O13	4e	0.6287(9)	0.3813(11)	0.6108(9)	0.038(2)
O14	4e	0.4095(10)	0.2791(12)	0.9575(8)	0.043(2)
S2	4e	0.9472(3)	0.3637(4)	0.3184(3)	0.0261(7)
O21	4e	0.9194(9)	0.2869(10)	0.1804(7)	0.0309(19)
O22	4e	0.0994(9)	0.4371(11)	0.3880(8)	0.034(2)
O23	4e	0.9385(9)	0.2434(10)	0.4222(8)	0.034(2)
O24	4e	0.8311(9)	0.4848(10)	0.2914(8)	0.035(2)
OW	4e	0.3293(9)	0.9235(10)	0.5541(8)	0.036(2)

Table 7

Anisotropic displacement parameters $U_{ij}/\text{\AA}^2$ for the atoms in $\text{KDy}(\text{SO}_4)_2 \cdot \text{H}_2\text{O}$.

Atom	U_{11}	U_{22}	U_{33}	U_{12}	U_{13}	U_{23}
Dy	0.0352(4)	0.0210(4)	0.0197(3)	0.0000(3)	0.0132(2)	0.0006(3)
K	0.058(2)	0.059(2)	0.0407(16)	0.0002(15)	0.0240(14)	0.0026(17)
S1	0.0420(17)	0.0240(18)	0.0195(13)	-0.0035(12)	0.0164(13)	-0.0051(14)
O11	0.039(5)	0.013(5)	0.027(4)	-0.001(3)	0.010(3)	-0.001(3)
O12	0.045(5)	0.034(6)	0.028(4)	0.000(4)	0.025(4)	-0.008(4)
O13	0.043(5)	0.038(6)	0.043(5)	-0.014(4)	0.030(4)	0.016(4)
O14	0.060(6)	0.038(6)	0.024(4)	0.007(4)	0.014(4)	0.005(5)
S2	0.0360(16)	0.0233(17)	0.0207(13)	-0.0031(12)	0.0153(12)	-0.0024(14)
O21	0.037(4)	0.041(5)	0.016(3)	-0.006(4)	0.014(3)	-0.008(4)
O22	0.039(5)	0.036(5)	0.026(4)	-0.009(4)	0.015(4)	-0.006(4)
O23	0.049(5)	0.032(6)	0.023(4)	0.004(4)	0.019(4)	-0.003(4)
O24	0.038(5)	0.027(5)	0.041(5)	0.006(4)	0.021(4)	0.002(4)
OW	0.056(5)	0.023(5)	0.031(4)	0.002(4)	0.024(4)	-0.009(4)

Table 8

Hydrogen-bonding geometry in $\text{KLa}(\text{SO}_4)_2 \cdot \text{H}_2\text{O}$, $\text{KSm}(\text{SO}_4)_2 \cdot \text{H}_2\text{O}$ and $\text{KDy}(\text{SO}_4)_2 \cdot \text{H}_2\text{O}$.

$D-H$	A	$d(D-H)/\text{\AA}$	$d(H-A)/\text{\AA}$	Angle(DHA)/°	$d(D-A)/\text{\AA}$
<i>KLa(SO₄)₂ · H₂O</i>					
OW-H	O1	0.87	2.41	162	3.26
OW-H	O4	0.87	2.48	128	3.09
OW-H	S	0.87	2.89	150	3.67
<i>KSm(SO₄)₂ · H₂O</i>					
OW-H1	O24	0.75(5)	2.33	151	3.01
OW-H1	S2	0.75(5)	2.99	122	3.45
OW-H2	O11	0.75(5)	2.29	148	2.94
<i>KDy(SO₄)₂ · H₂O</i>					
OW-H1	O22	1.20(6)	1.95	124	2.84
OW-H1	O14	1.20(6)	2.35	119	3.156
OW-H2	O24	1.20(6)	2.03	124	2.92
OW-H2	O13	1.20(6)	2.26	124	3.14

Table 9

Selected interatomic distances/ \AA and angles/° in $\text{KLa}(\text{SO}_4)_2 \cdot \text{H}_2\text{O}$, $\text{KSm}(\text{SO}_4)_2 \cdot \text{H}_2\text{O}$ and $\text{KDy}(\text{SO}_4)_2 \cdot \text{H}_2\text{O}$.

	$\text{KLa}(\text{SO}_4)_2 \cdot \text{H}_2\text{O}$	$\text{KSm}(\text{SO}_4)_2 \cdot \text{H}_2\text{O}$	$\text{KDy}(\text{SO}_4)_2 \cdot \text{H}_2\text{O}$
Ln-O	2.532(3)–2.623(3) (9 ×)	2.427(3)–2.865(5) (9 ×)	2.303(7)–2.560(8) (8 ×)
Ln-S	3.1985(8)	3.1480(13)–3.2488(13) (2 ×)	3.072(3)
K-O	2.546(3)–2.907(3) (8 ×)	2.767(5)–3.172(4) (9 ×)	2.673(9)–3.288(8) (9 ×)
K-S	3.4241(8)–3.7778(10) (4 ×)	3.5383(18)–3.7739(19) (3 ×)	3.538(4)–3.749(4) (3 ×)
S-O	1.463(3)–1.474(3) (4 ×)	1.447(4)–1.478(4) (8 ×)	1.452(7)–1.496(8) (8 ×)
O-Ln-O	53.82(9)–146.99(9)	51.68(13)–144.94(13)	56.8(3)–149.8(3)
O-K-O	49.61(8)–149.86(14)	43.99(9)–173.94(12)	43.1(2)–170.4(2)
O-S-O	104.94(15)–111.33(17)	105.5(2)–112.9(3)	105.7(5)–111.7(5)

atoms stemming from a bidentate sulphate ligand, five from monodentate sulphate ligands and the eighth from a crystal water molecule. The Ln -O distances are determined to lie between 2.427(3)–2.865(5) \AA in **1** and 2.303(7)–2.560(8) \AA in **2**. These distances agree well with the sum of the ionic radii of 2.44 (**1**) and 2.38 \AA (**2**) [19].

The difference in the coordination number of the Ln cation in both structures is due to a slight rotation of the sulphate ion (S1). Therefore, the Sm-O14 distance (2.86 \AA) is drastically shorter than Dy-O14 (3.54 \AA), which reduces the coordination number from nine (**1**) to eight (**2**). This is confirmed by corresponding MAPLE (MAdelung Part of Lattice Energy [20,21]) calculations (Table S1 in the Supplement) and the resulting effective coordination numbers (Table S2 in the Supplement). The calculations were performed for **1** (represented by the samarium compound) and **2** (Dy) on the basis of their refined crystal

structures. The MAPLE values of $\text{KSm}(\text{SO}_4)_2 \cdot \text{H}_2\text{O}$ and $\text{KDy}(\text{SO}_4)_2 \cdot \text{H}_2\text{O}$ differ from the sum of the MAPLE values of $\text{Sm}_2\text{O}_3/\text{Dy}_2\text{O}_3$ [22,23], SO_3 [24], $\text{K}_2\text{S}_2\text{O}_7$ [25] and hexagonal ice [26] only by 1.2% (**1**) and 0.1% (**2**).

Summarising **1** and **2**, the S-O distances in the SO_4^{2-} tetrahedra vary between 1.447(4) and 1.496(8) \AA , the O-S-O angles range from 105.5(2)° to 112.9(3)°. These distances agree well with the sum of ionic radii of 1.47 \AA [19], the bond angles reflect typical values for tetrahedra in crystalline compounds [27].

4. Crystal structure of $\text{KLa}(\text{SO}_4)_2 \cdot \text{H}_2\text{O}$

The crystal structure of $\text{KLa}(\text{SO}_4)_2 \cdot \text{H}_2\text{O}$ does not adopt one of the structures of the previously described $\text{KLn}(\text{SO}_4)_2 \cdot \text{H}_2\text{O}$ ($Ln=\text{Sm}, \text{Eu}, \text{Gd}, \text{Dy}$) but is isotypic with $\text{NaLn}(\text{SO}_4)_2 \cdot \text{H}_2\text{O}$ ($Ln=\text{Ce}$ [7], Gd [8])

crystallising in space group $P\bar{3}_121$ (no. 154). Thus the crystal structure of potassium lanthanum sulphate monohydrate is enantiomorphic with $\text{NaNd}(\text{SO}_4)_2 \cdot \text{H}_2\text{O}$ [8] and $\text{NaLa}(\text{SO}_4)_2 \cdot \text{H}_2\text{O}$ [9]

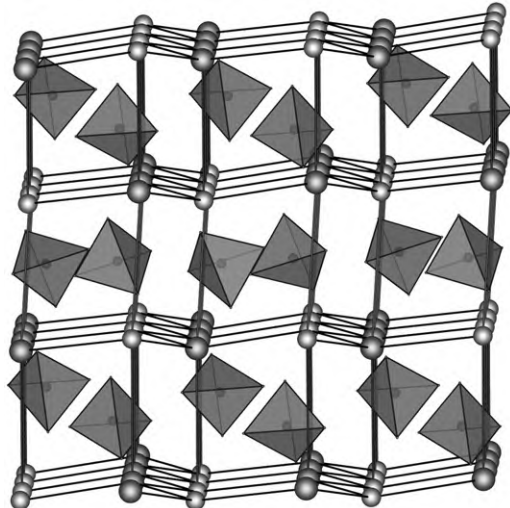


Fig. 1. Cation packing of $\text{KLn}(\text{SO}_4)_2 \cdot \text{H}_2\text{O}$ showing hexagonal undulated layers of alternating Ln (grey) and K (white) atoms perpendicular the bc -layer viewed along [010]. Between the layers the SO_4^{2-} tetrahedra (light grey) are located.

($P\bar{3}_121$). The cationic substructure consists of alternating K and La atoms forming undulated layers, the SO_4 tetrahedra and H_2O are located between the layers (Fig. 5).

The La and K environments can be described as $[\text{LaO}_9]$ polyhedra and $[\text{KO}_8]$ polyhedra [28]. The lanthanum atoms are nine-fold coordinated in the form of a distorted tricapped trigonal prism by eight O atoms of six SO_4^{2-} ions (two bideterminate and four monodeterminate) and a single crystal water molecule (Fig. 6). The $\text{La}-\text{O}$ distances vary from 2.532(3) to 2.623(3) Å. In contrast to **1** and **2** the K atoms are surrounded by eight sulphate oxygen atoms (Fig. 6). The S–O distances range from 1.463(3) to 1.474(3) Å, which is similar to **1** and **2**.

5. UV-vis spectroscopy of $\text{KLn}(\text{SO}_4)_2 \cdot \text{H}_2\text{O}$

The UV-vis spectra of $\text{KLn}(\text{SO}_4)_2 \cdot \text{H}_2\text{O}$ ($\text{Ln}=\text{Eu, Nd}$) are shown in Figs. 7 and 8. Therein all relevant $4f$ – $4f$ transitions are indicated according to the well known energy level schemes of both lanthanide ions [29]. In $\text{KEu}(\text{SO}_4)_2 \cdot \text{H}_2\text{O}$ all transitions start from the ground state 7F_0 , in $\text{KNd}(\text{SO}_4)_2 \cdot \text{H}_2\text{O}$ from the ground state ${}^4I_{9/2}$. Significant shifts of the emission lines relatively to the expected values could not be observed, the charge-transfer transition typical for Eu^{3+} is located at the minimum reflection at 254 nm which is a very common value for Eu^{3+} surrounded by oxygen atoms only.

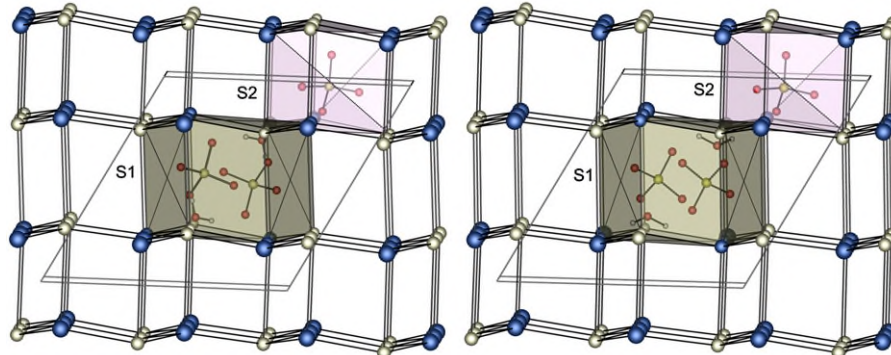


Fig. 2. Representation of the voids in $\text{KSm}(\text{SO}_4)_2 \cdot \text{H}_2\text{O}$ (**1**) (left) and in $\text{KDy}(\text{SO}_4)_2 \cdot \text{H}_2\text{O}$ (**2**) (right) seen along [010].

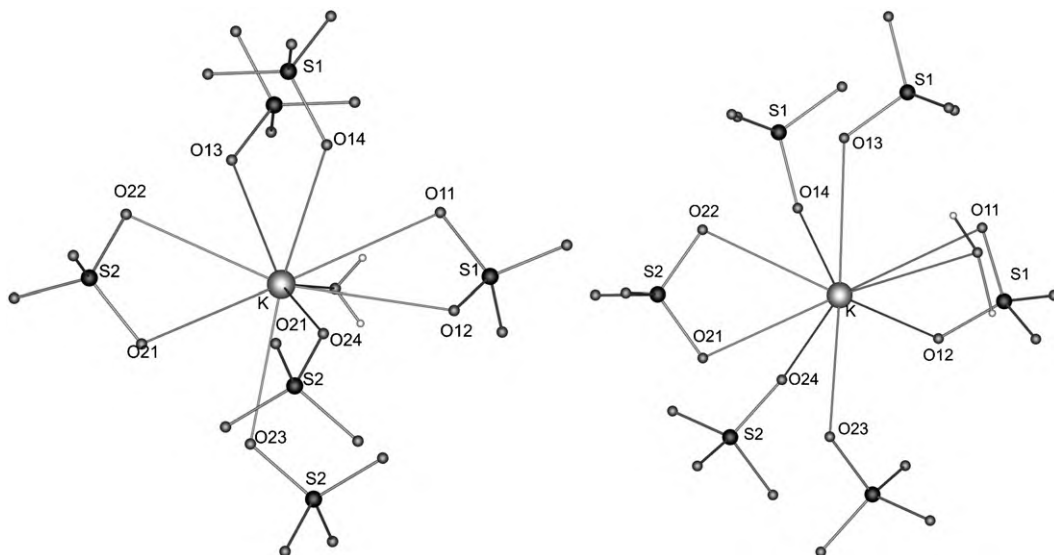


Fig. 3. Coordination geometry for the potassium ions in $\text{KSm}(\text{SO}_4)_2 \cdot \text{H}_2\text{O}$ (**1**) (left) and $\text{KDy}(\text{SO}_4)_2 \cdot \text{H}_2\text{O}$ (**2**) (right).

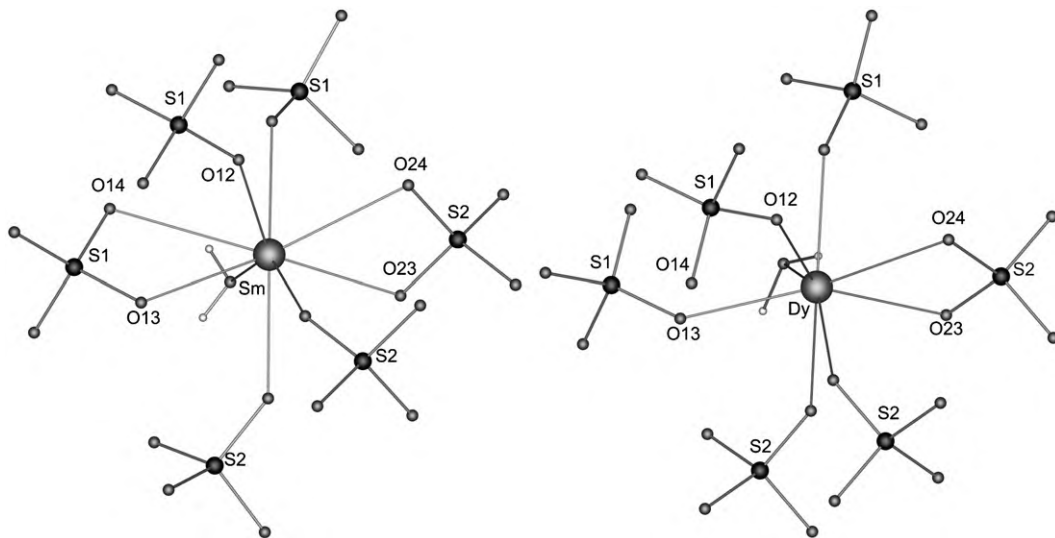


Fig. 4. Coordination environment of the lanthanide ions in KSm(SO₄)₂ · H₂O (**1**) (left) and KDy(SO₄)₂ · H₂O (**2**) (right).

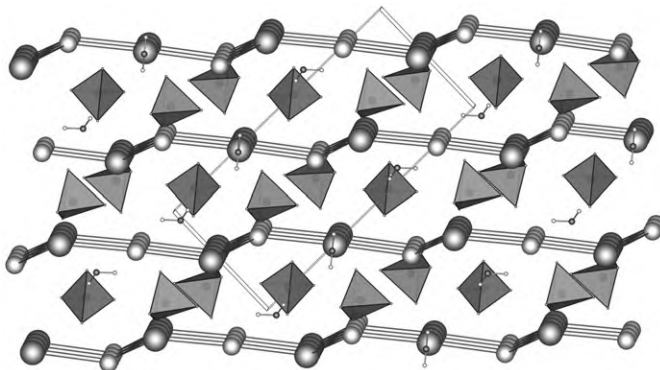


Fig. 5. Representation of the crystal structure of KLa(SO₄)₂ · H₂O along [010]. Light grey indicates La and white K atoms which form slightly undulated layers. Between the layers SO₄²⁻ tetrahedra (dark grey) and crystal water are localised.

6. Vibrational spectroscopy of $KLn(\text{SO}_4)_2 \cdot \text{H}_2\text{O}$

The infrared and Raman spectra of $KLn(\text{SO}_4)_2 \cdot \text{H}_2\text{O}$ ($Ln=\text{La}$ (**a**), Sm (**b**), Dy (**c**)) are shown in Fig. 9, thus each structure type is represented by one example. The infrared spectra of the three compounds are similar. The absorption from 3800 to 2600 cm⁻¹ is assigned to O-H stretching vibrations ($\nu(\text{OH})$) of water molecules affected by hydrogen bonding. A weak band is observed at 1680 cm⁻¹ for (**a**) and (**c**), attributable to the bending modes ($\sigma(\text{OH})$) of a water molecule. The vibrations of the inorganic free SO₄²⁻ ion are observed between 1450 and 400 cm⁻¹ [30]. The characteristic peaks of the $\nu_{as}(\text{SO}_4)$ stretching modes are excited at 1180 cm⁻¹ (**a**), 1150 cm⁻¹ (**b**), 1120 cm⁻¹ (**c**). The Sm, Dy and La double sulphates show IR peaks in the region between 890 and 880 cm⁻¹ (**a-c**), which can be assigned to symmetric stretching vibration of the free SO₄²⁻ anion [31]. The bending mode ($\delta_{as}(\text{SO}_4)$) of sulphates occurs around 600 cm⁻¹ [32]. The symmetric S-O bending vibrations of the SO₄²⁻ ion appear in the 520–400 cm⁻¹ region.

The Raman spectra show intense peaks between 1280 and 400 cm⁻¹. The three strongest emissions around 1130, 1050 and 1000 cm⁻¹ originate from asymmetric stretching vibrations. The emission between 640 and 400 cm⁻¹ can be attributed to

the bending vibration of the SO₄²⁻ ions. Thus the observed frequencies in the spectra correspond very well with the expected values and our structure models.

7. Conclusion and discussion

Observed structural differences in homologous series of lanthanide compounds are normally due to the evolution of the ionic radii or special electronic properties like semi-filled or fully occupied 4f states. Frequently, the coordination number tends to be reduced starting from the larger lanthanides going to the smaller ones.

In this contribution we determined the crystal structures of $KLn(\text{SO}_4)_2 \cdot \text{H}_2\text{O}$ ($Ln=\text{La}, \text{Nd}, \text{Sm}, \text{Eu}, \text{Gd}, \text{Dy}$) and found that KLa(SO₄)₂ · H₂O (**3**) and $KLn(\text{SO}_4)_2 \cdot \text{H}_2\text{O}$ ($Ln=\text{Nd}, \text{Sm}, \text{Eu}, \text{Gd}, \text{Dy}$) crystallise in different structure types. This is not further surprising since La is significantly larger compared with the other mentioned lanthanides. La is coordinated by nine oxygen atoms, which is partially also found for the other $KLn(\text{SO}_4)_2 \cdot \text{H}_2\text{O}$.

On a first sight the remaining $KLn(\text{SO}_4)_2 \cdot \text{H}_2\text{O}$ with $Ln=\text{Ce}$ (type **1**, [10]), Pr (type **2**, [11]), Nd (**1**, this work), Sm (**1**, this work), Eu (**2**, this work), Gd (**1**, this work), Tb (**2**, [12]), Dy (**2**, this work) and Lu (**2**, [13]) might be considered to be isotypic. But a closer look reveals that the slight rotation of a sulphate anion reduces the coordination number around the lanthanide (**1**, $Ln=\text{Ce}, \text{Nd}, \text{Sm}, \text{Gd}$) from nine to eight (**2**, $Ln=\text{Pr}, \text{Eu}, \text{Dy}, \text{Lu}$). This is unexpected since the ionic radii decrease along the series Ce, Pr, Nd, Sm, Eu, Gd, Tb, Dy and Lu. Extending the view to the whole series of similar compounds characterised so far, an average trend to a smaller coordination number as expected is found. Maybe the differences between both forms are very small and both forms might be observed depending on the synthesis conditions, although we did not observe the coexistence of both phases so far. The cell parameters of these compounds show the normal decrease according to the lanthanoids' contraction very clearly only along the *b*-axis while the *c*-axis lengths are rather similar and the *a*-axis values do not show a clear trend. Thus, also from the cell parameters no indication for the coordination switch can be deduced.

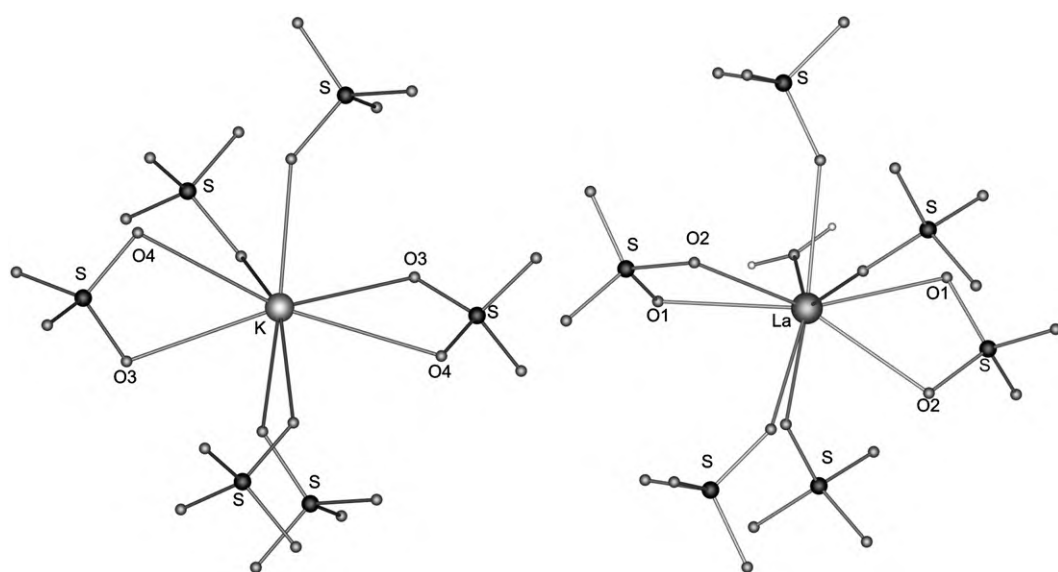


Fig. 6. Coordination environment of the K (left) and La atoms (right) in $\text{KLa}(\text{SO}_4)_2 \cdot \text{H}_2\text{O}$.

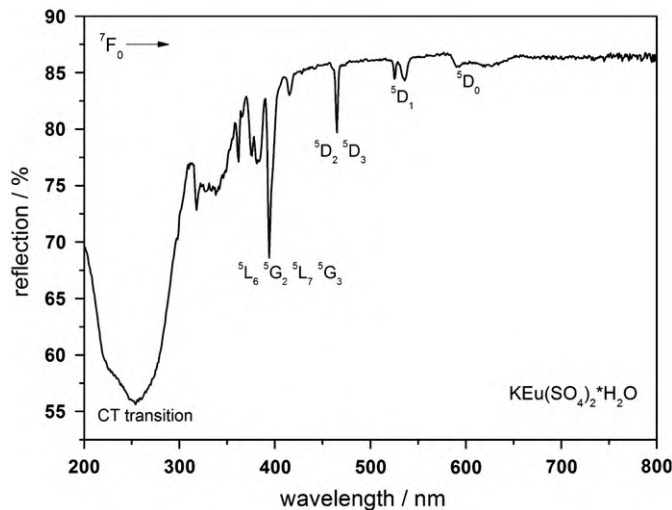


Fig. 7. UV-vis reflection spectrum of $\text{KEu}(\text{SO}_4)_2 \cdot \text{H}_2\text{O}$; all relevant transitions have been indicated.

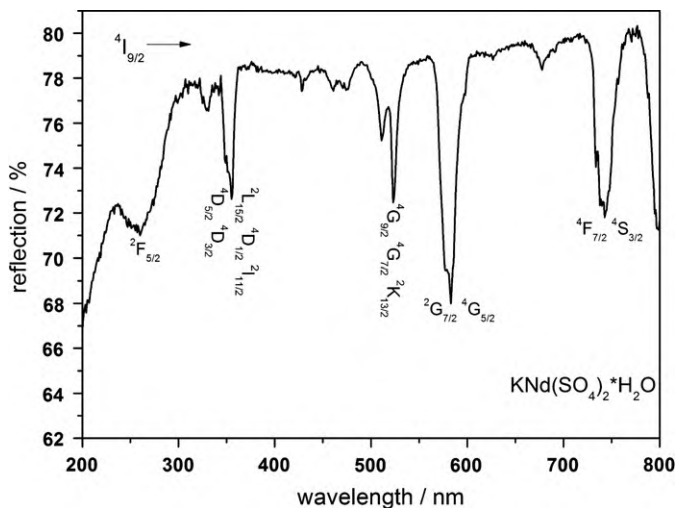


Fig. 8. UV-vis reflection spectrum of $\text{KNd}(\text{SO}_4)_2 \cdot \text{H}_2\text{O}$; all relevant transitions have been indicated.

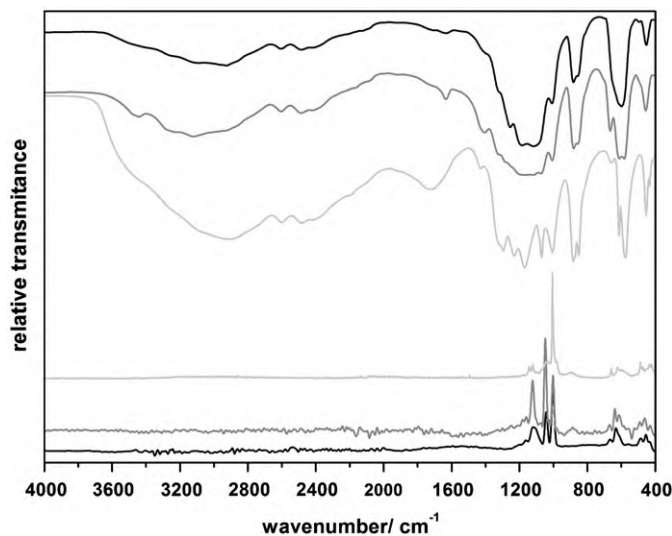


Fig. 9. Infrared and Raman spectra of $\text{KSm}(\text{SO}_4)_2 \cdot \text{H}_2\text{O}$ (black), $\text{KDy}(\text{SO}_4)_2 \cdot \text{H}_2\text{O}$ (dark grey) and $\text{KLa}(\text{SO}_4)_2 \cdot \text{H}_2\text{O}$ (light grey).

Acknowledgments

The authors thank Prof. Dr. H. Hillebrecht, Albert-Ludwigs-Universität Freiburg, for valuable discussions and generous support. Financial support by the Fonds der Chemischen Industrie (H.A.H.: Liebig Habilitationsstipendium; K.K.: Doktorandenstipendium) is gratefully acknowledged.

Appendix A. Supplementary material

Supplementary data associated with this article can be found in the online version at doi:10.1016/j.jssc.2010.07.024.

References

- [1] (a) T. Jüstel, H. Nikol, C. Ronda, Angew. Chem. Int. Ed. 37 (1998) 3084;
(b) H.A. Höpke, Angew. Chem. Int. Ed. 48 (2009) 3572.

- [2] (a) P.C. Junk, C.J. Kepert, B.W. Skelton, A.H. White, *Austr. J. Chem.* 52 (1999) 601;
 (b) M.S. Wickleder, *Z. Anorg. Allg. Chem.* 625 (1999) 1548.
- [3] M.S. Wickleder, *Chem. Rev.* 102 (2002) 2011.
- [4] P.D. Robinson, S. Jasty, *Acta Crystallogr. C54* (1998) 1.
- [5] N.L. Sarukhanyan, L.D. Iskhakova, V.K. Trunov, V.V. Ilyukhin, *Coord. Chem. USSR* 10 (1984) 981.
- [6] L.D. Iskhakova, S.A. Bondar, V.K. Trunov, *Kristallografiya* 32 (1987) 328.
- [7] A.C. Blackburn, R.E. Gerkin, *Acta Crystallogr. C51* (1995) 2215.
- [8] J. Perles, C. Fortes-Revilla, E. Gutiérrez-Puebla, M. Iglesias, M. Monge, C. Ruiz-Valero, N. Snejko, *Chem. Mater.* 17 (2005) 2701.
- [9] A.C. Blackburn, R.E. Gerkin, *Acta Crystallogr. C50* (1994) 835.
- [10] M. Jemmalí, S. Walha, R.B. Hassen, P. Vaclac, *Acta Crystallogr. C61* (2005) i73.
- [11] L.D. Iskhakova, N.L. Sarukhanyan, T.M. Shchegoleva, V.K. Trunov, *Kristallografiya* 30 (1985) 474.
- [12] V.I. Lyutin, Yu.N. Safyanov, E.A. Kuz'min, V.V. Ilyukhin, N.V. Belov, *Kristallografiya* 19 (1974) 376.
- [13] N.L. Sarukhanyan, L.D. Iskhakova, I.G. Drobinskaya, V.K. Trunov, *Kristallografiya* 30 (1985) 880.
- [14] Stoe & Cie (Darmstadt), Programs X-Red and X-SHAPE, 1999.
- [15] T. Higashi, ABSCOR Rigaku Corporation, Tokyo, Japan, 1995.
- [16] SADABS: Area-Detector Absorption Correction, Siemens Industrial Automation Inc., Madison, WI, 1996.
- [17] G.M. Sheldrick, V. SHELXTL, in: 5.10 Crystallographic System, Bruker AXS, Analytical X-ray Instruments Inc., Madison, 1997.
- [18] R.S. Pease, *Acta Crystallogr. 5* (1952) 356.
- [19] D. Shannon, C.T. Prewitt, *Acta Crystallogr. B25* (1969) 925.
- [20] (a) R. Hoppe, *Angew. Chem. Int. Ed. Engl.* 5 (1966) 95;
 (b) R. Hoppe, *Angew. Chem. Int. Ed. Engl.* 9 (1970) 25.
- [21] R. Hübenthal, MAPLE, Program for the Calculation of the Madelung Part of Lattice Energy, 1993.
- [22] F. Hanic, M. Hartmanová, G.G. Knab, A.A. Urusovskaya, K.S. Bagdasarov, *Acta Crystallogr. B40* (1984) 76.
- [23] E.N. Maslen, V.A. Streletsov, N. Ishizawa, *Acta Crystallogr. B52* (1996) 411.
- [24] W.S. McDonald, D.W.J. Cruickshank, *Acta Crystallogr. B22* (1967) 48.
- [25] K. Stahl, T. Balic-Zunic, F. da Silva, K.M. Eriksen, R.W. Berg, R. Fehrmann, *J. Solid State Chem.* 178 (2005) 1697.
- [26] A. Goto, T. Hondoh, S. Mae, *J. Chem. Phys.* 93 (1990) 1412.
- [27] S.J. Louisnathan, R.J. Hill, G.V. Gibbs, *Phys. Chem. Miner.* 1 (1977) 53.
- [28] Again, a precise look on the original data in Ref. [7] revealed that the Na atoms are not six-fold but eight-fold coordinated.
- [29] G.H. Dieke, in: *Spectra and Energy Levels of Rare Earth Ions in Crystals*, John Wiley & Sons, London, 1968.
- [30] J.T. Kloprogge, H. Ruan, L.V. Duong, R.L. Frost, Neth. *J. Geosci.* 80 (2001) 41.
- [31] J. Baran, M.M. Ilczyszyn, M.K. Marchewka, H. Ratajczak, *Spectrosc. Lett.* 32 (1) (1999) 83.
- [32] C. Posmus, J.R. Ferraro, *J. Chem. Phys.* 48 (1968) 3605.